Design of Acoustic Linings for Ducts with Flow

WALTER EVERSMAN*
The Boeing Company and Wichita State University, Wichita, Kansas
AND
M. DEAN NELSEN,† DENIS ARMSTRONG,‡ ORVILLE J. HALL JR.§
The Boeing Company, Wichita, Kansas

A procedure for the design of acoustic linings for the attenuation of fan generated noise in turbo fan engines is described. This procedure is based on an interaction between an extensive analytical lining performance prediction capability and flow duct testing. The theoretical basis for lining analysis in rectangular, circular, and annular ducts with either uniform or sheared flow is formulated and the results of the development of a lining mathematical model are presented. The predictive capability is employed in conjunction with a least attenuated mode lining optimization scheme to determine the lining impedance which will provide the required attenuation spectrum. A flow duct test facility is briefly described and results of the testing of lining designs and the comparison with theoretical predictions is presented.

Introduction

IN response to recently enacted regulations,[1] powerplant and airframe manufacturers have begun a program to substantially reduce the noise of conventional and turbo-fan engines. Success in jet noise suppression has lowered the noise floor sufficiently that the reduction of fan and compressor noise has become a major consideration.

The technique for achieving fan noise reduction can be broken down into two distinct approaches. One method consists of reduction of the noise at the source. This is to be accomplished by the development of a detailed understanding of the noise generation mechanism in the fan stages and the use of this knowledge to design fans and compressors which operate at reduced noise levels. The second method accepts the presence of the noise source and seeks to attenuate the sound in the fan inlet and exhaust ducts by acoustic treatment of the duct walls. The present paper deals with the second approach and details the elements of a theoretical and experimental program for duct lining design and optimization.

The theoretical analysis and prediction of the performance of acoustic lining materials in an actual engine application is made difficult and costly by the complicated duct geometries and operating conditions which are encountered. Exact theoretical analysis is not practical and experimental work under full-scale operating conditions, although necessary for final design verification, is too costly for developmental work aimed at optimization of lining configurations. For these reasons, the study of lining materials is generally based on simplified, but representative, mathematical models and by experimental investigations in flow ducts which roughly match the conditions found in actual fan inlet and exhaust ducts.

Theoretical and experimental investigations of the transmission and attenuation of sound in ducts has been a field of fruitful research for a number of years. Original interest was directed toward the transmission of noise in air distribution systems, but aircraft applications have intensified the interest in recent years and a substantial basis of experimental and theoretical results is being developed.

Experimental programs for lining development and sound transmission investigations have appeared in the literature[2-5] as have descriptions of facilities for systematic testing.[6-8] Much of the test work was carried out before an extensive theoretical model was available for the prediction of duct lining performance. However, mathematical modeling of the sound transmission in ducts with and without flow[9-18] has reached a high state of development and is available for design computations.

The modeling of the acoustic lining has been a more difficult process. The description of acoustic linings has generally been accomplished by experimental means involving steady flow resistance testing and standing wave tube tests. Results of this type of testing are available from lining suppliers and have been reported in the literature, as by Marsh.[6] Mathematical models have depended heavily on empirical models based on the steady flow resistance work of Green and Duwez[19] for porous media, Beranek's oscillatory flow resistance work for perforated sheet,[20] and studies of the behavior of Helmholtz resonators, such as by Phillips.[21] A major portion of the investigation described in the present paper has been directed toward developing a lining impedance model, based on the above studies, which accurately accounts for steady and oscillatory viscous effects, grazing flow effects, and inertial effects.

Lining Design and Optimization Procedure

The parameters which control the design of an acoustic lining include: engine performance data (duct flow conditions); geometry (duct size and allowable lining length); and acoustic objectives (amount of attenuation and frequency bandwidths requiring attenuation). Of these parameters, engine performance data and geometry can be considered relatively well defined, while the establishment of acoustic objectives can be considered a major step in the design process.

The first phase of the lining design procedure is the establishment of the design objectives. This phase begins with the acquisition of the $\frac{1}{3}$ octave far field and the 100 Hz narrow band near field (fan inlet and exhaust duct) noise signatures of the subject engine. These data are obtained from full-scale engine testing. Data are taken for approach, cutback, and takeoff engine conditions. The far field polar data are

Presented as Paper 71-731 at the AIAA 7th Propulsion Joint Specialist Conference; submitted April 9, 1972, revision received April 14, 1972. Portions of the development effort described in this paper were accomplished with the support of NASA Lewis Research Center. Thanks are due to Pratt and Whitney Aircraft and Brunswick Corporation, Metal Fibers-Technical Production Division for permission to make use of data referred to in this paper.

Index categories: Aerodynamic and Powerplant Noise (Including Sonic Boom); Aircraft Propulsion System Noise.

* Consultant and Associate Professor. Member AIAA.
† Manager, Nacelle Technology. Member AIAA.
‡ Engineer.
§ Senior Engineer.

separated into components representing fan noise, primary jet noise, secondary jet (fan discharge) noise, and turbomachinery noise, and input to an effective perceived noise level (EPNL) program which predicts EPNL values for fixed observer locations with a given aircraft flight path. Trade studies are made for combinations of fan inlet and exhaust attenuations (based on normalized attenuation spectra synthesized from accumulated lining design experience) until an acceptable EPNL level is achieved. This process will define an objective far field attenuation spectrum and will define attenuation spectra for the far field noise from the inlet and exhaust ducts. The attenuation objectives may fall below jet noise and turbomachinery noise floors in anticipation of improvements in these areas.

The far field attenuation objectives are then applied directly to the near field data, after these data are transformed to $\frac{1}{3}$ octave. These spectra, in addition to pure tone spikes which can only be seen in the narrow band data, furnish objectives to which the duct lining design procedure will be addressed. Since this process can be repeated for approach, cutback, and takeoff conditions, the design objectives for the individual cases will be compromised to form a composite design objective for fan inlet and exhaust linings. The design objectives can be briefly described as specifying certain target frequencies at which the lining performance is to be optimized (generally pure tone spikes) as well as broad band attenuation requirements.

The analytical design phase depends on three types of computer programs. These are: a) duct propagation based on uniform flow assumption (UF), b) duct propagation based on sheared flow (boundary layer) model (SF), c) lining material properties program (MP). The design philosophy is based on a least attenuated mode concept and is most appropriate for ducts with a fairly large length to width ratio. A multimodal approach would be required for short ducts. In the least attenuated mode concept the lining is optimized at a target frequency in such a way that the least attenuated mode has the greatest attenuation possible. This is accomplished using both UF and SF. The resulting optimum installed impedance is translated into lining parameters via MP. Given the resulting optimum impedance a multimodal version of either UF or SF is used to generate an attenuation spectrum. The attenuation spectrum objective is met by choosing optimum impedances (several lining sections of different impedance or a multiple degree of freedom lining may be dictated if there is more than one target frequency) and appropriate lining lengths. Once a design is determined, allowable manufacturing tolerances for the lining are established by parametric variations using UF. Design verification is then accomplished by flow duct testing.

In the preceeding discussion we have indicated the existence of an analytical and experimental capability for the analysis and design of acoustic lining for ducts. It is the purpose of this paper to present the details of the test facility and mathematical models employed in the design and analysis procedure and to indicate by specific examples the success with which we have been able to mathematically model acoustic lining behavior.

Flow Duct Test Facility

The Boeing-Wichita acoustic flow duct test facility was developed to simulate the aerodynamic and acoustic properties of both the inlet and exhaust fan ducts on fanjet engines. As shown in Fig. 1, this facility is of the double reverberant chamber type discussed by Melling and Doak.[8] The two acoustic reverberation chambers are utilized at each end of the test section to provide diffuse sound fields for the determination of the acoustic performance of the lining material and act as plenums for the air flow through the test section. They are defined as primary and secondary chambers. The primary chamber is connected directly to the inlet and exhaust mode ejector systems. In the exhaust mode of operation, the sound and air flow both originate in the primary chamber. In the inlet mode of operation the sound is generated in the primary chamber while the air flow is drawn in the opposite direction from the secondary chamber by an ejector system.

The test section is a unique design which will permit the duct geometry to be easily and rapidly changed to meet specific requirements. These geometric changes may be accomplished during normal panel changes or while the duct is operating. Acoustically treated test panels and solid aluminum blanking panels are fitted into the walls of the test section.

Several types of acoustic generators are available to produce the desired sonic spectrums, but the prime source is the noise generated from the air ejector and plumbing systems. A degree of level control on this acoustic energy may be obtained by balancing and simultaneously operating the inlet and exhaust mode ejectors, thus producing higher sound levels at the lower Mach number flow conditions. Auxiliary noise generators are located in the primary chamber to supplement the ejector in the higher frequencies. The noise generators consist of impinging air jets and nozzles, a discrete frequency siren capable of 160 to 170 db from 1500 Hz to 4000 Hz, and a 140 db tunable Hartman generator whistle.

The performance of acoustic linings is generally monitored in terms of the insertion loss spectrum of the lining. The insertion loss is obtained by testing with and without lining

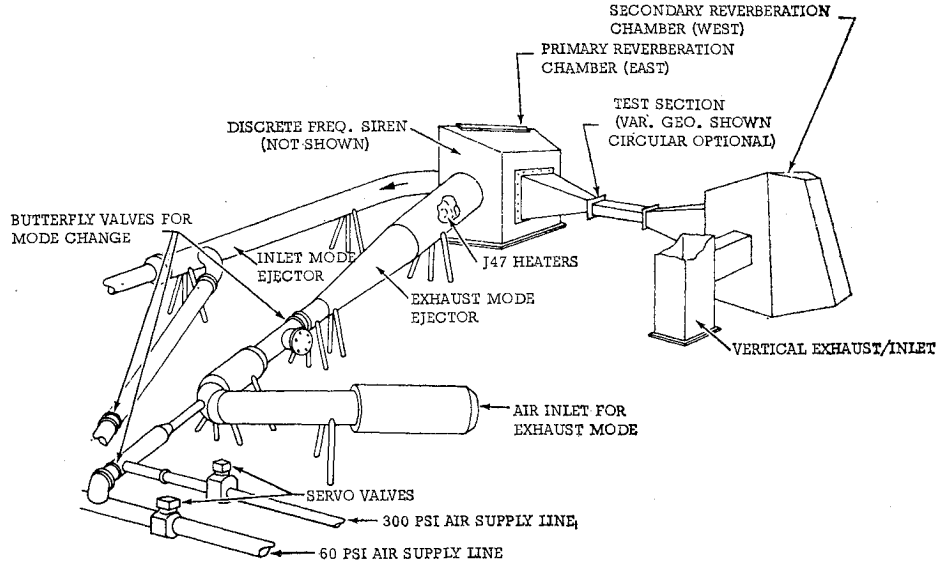

Fig. 1 Sketch of flow duct.

Table 1 Boeing-Wichita flow duct characteristics

Parameter	Inlet/exhaust mode
Mach Number	0.40/0.60
Sound pressure level	155/160 db over-all
Discrete frequency sonic generator	500*5000 Hz

material. A baseline test is performed using hard wall aluminum blanking panels with the acoustic spectrum being recorded in both the primary and secondary chambers for a series of Mach numbers in both the inlet and exhaust modes of operation. The test is then repeated using the subject test panels. The insertion loss in each test condition is determined as the difference between the acoustic spectrum in the secondary chamber with and without lining material. In addition, flush mounted microphones are located throughout the length of the lining so that the rates of acoustic attenuation can be computed.

The important performance characteristics of the Boeing-Wichita flow duct facility are given in Table 1.

Lining Model

A theoretical calculation of the transmission of sound in a lined duct with flow requires a detailed description of the impedance of the lined walls. The installed impedance of the lined walls provides the necessary boundary condition for the transmission calculation.

The lined walls are typically constructed as shown in Fig. 2. The liner consists of arrays of normally reacting Helmholtz resonators provided by small cavities sandwiched between a porous face sheet and impervious backing. The impedance of the liner may be expressed as

$$\frac{Z}{\rho c} = \left[\frac{R}{\rho c} + i\frac{X}{\rho c}\right]_{\text{face sheet}} - \left[i\cot\frac{2\pi fd}{c}\right]_{\text{cavity}} \tag{1}$$

provided that all dimensions are small with respect to wavelength. In Eq. (1) ρ is the fluid density, c the speed of sound, R and X the resistive and reactive components of the face sheet impedance, f the driving frequency in Hz and d the backing space depth.

Many studies are reported in the literature which describe the acoustic behavior of the liner face sheet. These theoretical and experimental studies have been conducted on both perforated and fibrous materials. Until recent years the studies have been directed primarily to the "linear" acoustic regime for the case where no fluid flow is grazing the acoustic liner. Beranek[20] has summarized many of the results of such studies.

With the advent of serious development of the rocket engine and the need for sound absorption in the flow passages of the gas turbine engine, many additional impedance studies have been conducted. Studies such as those of Zinn,[22] Blackman,[21] Garrison,[23] Fedder and Dean[24] have investigated acoustic impedance in the "nonlinear" regime with specific emphasis on the effects of grazing flow.

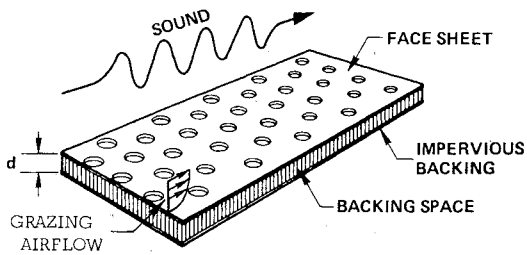

Fig. 2 Typical lining configuration.

The first step in modeling the resistance component of the face sheet impedance is accomplished by isolating the dissipation mechanism for steady flow conditions in terms of the fluid properties, face sheet geometry, and particle flow. The isothermal, one-dimensional, steady flow pressure loss of a fluid flowing through a homogeneous porous matrix, Fig. 3, has been mathematically described by Green and Duwez[18] as

$$(P_1^2 - P_2^2)/2bTt = \alpha\mu G + \left(\beta + \frac{1}{t}\ln\frac{P_1}{P_2}\right)G^2 \tag{2}$$

where $G = \rho_1 V_1 = \rho_2 V_2$, μ is the absolute viscosity of the fluid, b is the gas constant in $PV = bT$. α is the viscous (linear) loss coefficient and β the inertial (nonlinear) loss coefficient, both of which are dependent on material geometry only. The ratio β/α, as described by Green and Duwez, is the characteristic length which represents the dissipative characteristics of a particular matrix.

For the small pressure gradients imposed in acoustic applications, the equation can be simplified and arranged to yield the steady flow (D.C.) resistance of the material

$$R_{\text{D.C.}} = \Delta P/V_P = R_{V\text{D.C.}} + R_{I\text{D.C.}} \tag{3}$$

where

$$R_{V\text{D.C.}} = \alpha\mu t \quad \text{(viscous resistance)} \tag{3b}$$

$$R_{I\text{D.C.}} = \beta\rho t V_P \quad \text{(inertial resistance)} \tag{3c}$$

Equation (3) clearly indicates that the non-linearity of a homogeneous material is related to the characteristic dimension (β/α) and the kinematic viscosity (μ/ρ) of the fluid. For the case of materials such as perforated sheet, Eq. (3c) must be modified as follows

$$R_{I\text{D.C.}} = \bar{\beta}\rho V_P \tag{4}$$

since the inertial loss mechanism, being essentially independent of material thickness, occurs as a result of the sudden expansion as the fluid emerges from each perforation.

Equation (3) is transformed to the low-frequency acoustic regime by tracing the instantaneous resistance variation over a single period for a sinusoidaly applied pressure. The equivalent resistance is defined as the factor of proportionality which relates rms pressure loss to rms particle velocity $V_{P\text{rms}}$. This treatment is analogous to the theory of nonlinear resistance in electrical circuits and yields approximately

$$R_{\text{A.C.}} = \alpha\mu t + \frac{\pi}{2\sqrt{(2)^{1/2}}}\beta\rho t\, V_{P\text{rms}} \tag{5}$$

where α and β are computed from D.C. measurements from Eq. (3).

The last step in defining the acoustic resistance at zero grazing flow is to account for the variation in the dissipation

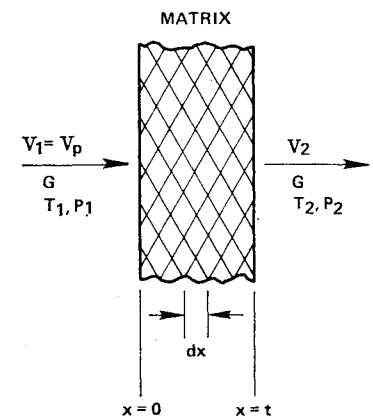

Fig. 3 Element of porous matrix.

mechanisms. The viscous resistance for certain materials increases with frequency by $(\Delta R_V)_{A.C.}$ due to additional shear produced by the alternating flow.[20] Analysis of standing wave impedance tube data for certain materials indicates the strength of the inertial loss mechanism depends on the amplitude of particle displacement and must be altered by a correction of functional form $\Phi(fl/VP_{rms})$ where l is the effective thickness of the material. This correction factor is found by empirical correlation of test data for particular materials.

Many investigators have shown that grazing airflow significantly affects the installed resistance of certain face sheet materials. The change in resistance ΔR_G due to grazing flow is intimately related to the viscous and inertial coefficients α and β, grazing flow Mach number, and the size and shape of the boundary layer as well as the surface roughness of the panel. If one assumes that the grazing flow induces local boundary-layer separation and related nonsteady low-frequency (nonacoustic) flow within the face sheet, an equivalent, non-resistance dependent RMS pressure fluctuation ΔP_{rms} can be related to the grazing flow dynamic pressure as

$$\Delta P_{\text{rms}} = K\tfrac{1}{2}\rho V_\infty{}^2 \tag{6}$$

where K is a function of the grazing flow boundary layer, face sheet surface geometry, and roughness, determined empirically. Equations (5) and (6) can be used to define an increment in rms particle velocity due to the grazing flow. This, in turn, can be employed in Eq. (5) to deduce an increment in the resistance due to the grazing flow. The change in normalized resistance $(\Delta R_G/\rho C)$ due to grazing airflow can be calculated as

$$\frac{\Delta R_G}{\rho C} = -\frac{\alpha\mu t}{2\rho C} + \left[\left(\frac{\alpha\mu t}{2\rho C}\right)^2 + \frac{\pi K}{4(\sqrt{2})^{1/2}}\beta t M_\infty{}^2\right]^{1/2} \tag{7}$$

Of particular interest in Eq. (7) are the limiting cases. For linear materials where $\alpha \gg \beta$ the grazing airflow provides no change in the installed resistance. For very nonlinear materials

$$\Delta R_G/\rho C = (M_\infty/2)\,[\pi K\beta T/(2)^{1/2}]^{1/2} \tag{7a}$$

Thus, very nonlinear materials can be expected to yield large resistance changes proportional to grazing flow Mach number.

Accounting for all of the observed phenomena $R/\rho C$ in Eq. (1) may be approximately computed by the following simplified superposition model for a given frequency

$$\frac{R}{\rho C} = \left(\frac{R_v}{\rho C}\right)_{D.C.} + \left(\frac{\Delta R_V}{\rho C}\right)_{A.C.} + \frac{\Delta R_G}{\rho C} + \frac{\pi}{2(2)^{1/2}}\frac{\beta t}{C} V_{P\text{rms}}\,\Phi(fl/V_{P\text{rms}}) \tag{8}$$

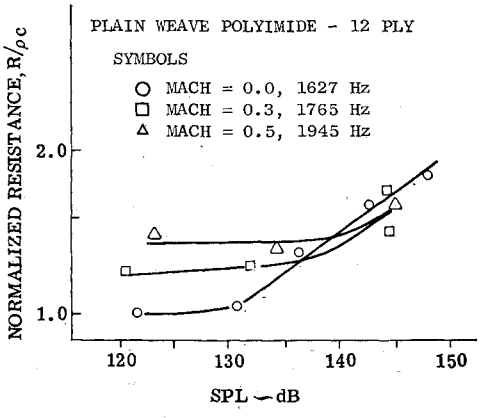

Fig. 4 Resistance of polyimide face sheet showing nonlinear behavior at high SPL and grazing flow effect.

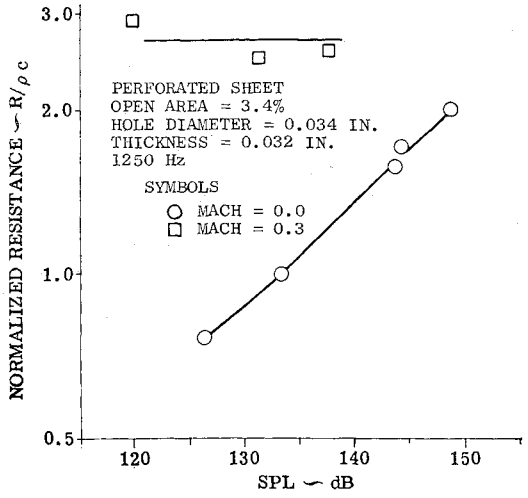

Fig. 5 Resistance of perforated sheet showing nonlinearity at zero grazing flow and transition to linear behavior with increase in grazing flow.

The elements of Eq. (8) can be best illustrated by the resistive impedance data shown in Figs. 4 and 5. Figure 4 shows data obtained from the Boeing-Wichita grazing flow wave-guide[25] for a polyimide face sheet material. By noting that the driving SPL is directly related to the particle velocity, the nonlinear characteristic of the material at high SPL (particle velocity) is seen. The linear (viscous) resistance predominates at low SPL whereas the nonlinear (inertial) resistance predominates at high SPL. As predicted by the mathematical model, when grazing flow increases the apparent linearity of the material is maintained to a significantly higher SPL. Similar data for a highly nonlinear perforated face sheet is shown in Fig. 5. In this case the viscous contribution is very small and is not detectable over the range of data shown. With a grazing flow Mach number of 0.3 the resistance of the material is dominated by the grazing flow effect to a point that linearity exists for a range of SPL's in excess of 150 db. Thus, we note the paradoxical behavior of highly nonlinear materials in the presence of grazing airflow.

The reactive impedance of the face sheet, $X/\rho C$ in Eq. (1), is computed using the classical fluid piston model modified to include the effects of particle velocity and grazing flow as follows:

$$X = 2\pi f M_A \tag{9}$$

where the piston mass M_A is given by

$$M_A = \rho_\sigma(t + \Delta t) \tag{10}$$

σ is the porosity of the face sheet, and $(t + \Delta t)$ is the effective length of the fluid piston. The excess length of the fluid piston (Δt) is functionally dependent upon particle velocity and grazing flow. An example of a complete mathematical model for a perforated plate lining can be found in Ref. (26).

As an indication of the validity of the mathematical model we have compared results computed from it with measured impedances of perforated sheet as reported by Garrison.[23] These results are at zero grazing flow and are shown in Fig. 6. To show the grazing flow effect we have compared the model to perforated plate data obtained by Feder and Dean.[24] Figure 7 shows these results using computed values at a hole diameter of 0.087 in. while the experimental results are for a range of hole diameters from 0.023 to 0.125 in. The empirical portions of the mathematical model were obtained independently of the data shown in these figures.

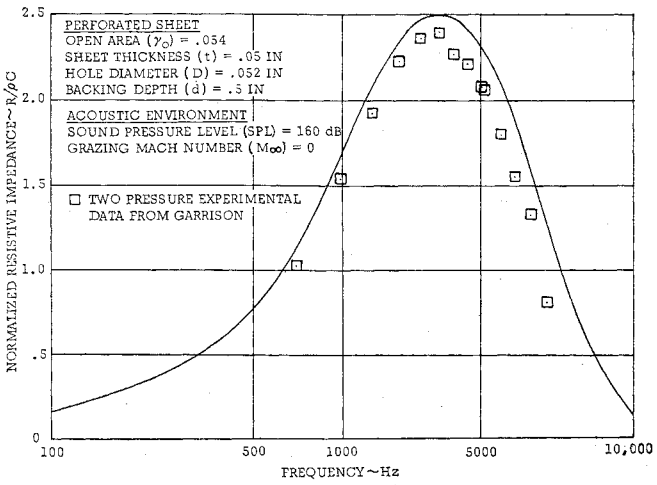

Fig. 6 Zero grazing flow comparison of theoretical and experimental results for resistive impedance of perforated sheet.

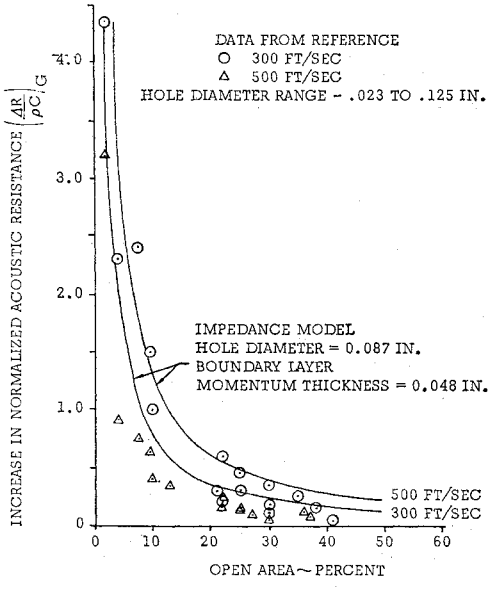

Fig. 7 A comparison of theoretical and experimental results for resistance change due to grazing flow.

Theoretical Analysis

Mathematical Model

In order to provide some measure of quantitative theoretical capability for the prediction of lining performance in ducts, a highly idealized mathematical model is employed.

The duct flow is modeled as flow of air in an infinite duct of rectangular, circular or annular cross section. Propagation is modeled according to the usual acoustic assumptions. Two types of mean flow can be employed. The simplest model assumes that the flow is uniform on the duct cross section so that the propagation of sound is governed by the convected wave equation. The second, more refined model, allows for an arbitrary sheared flow profile which can be employed to approximate the effect of boundary layer on sound transmission.

Uniform Flow Profile

The mathematical model employing a uniform flow profile is the primary tool for lining design and optimization because of computational economy. If the x axis is taken parallel to the axis of the duct, the propagation of pressure disturbances in the duct is governed by the convected wave equation

$$\nabla^2\rho - (1/C^2)[\partial/\partial t + u\partial/\partial x]^2\rho = 0 \tag{11}$$

Although parallel capability is available for rectangular, circular, and annular ducts with any combination of lined and unlined walls, the major testing and theoretical effort has been directed toward the rectangular duct with two opposite walls lined with the same material or with only one wall lined. Solutions for harmonic wave propagation in the m, n mode in the rectangular duct which satisfy the hard wall condition at $z = 0$ and $z = b$ are

$$\rho_{mn} = e^{i(\omega t - k_{xmn}x)}\,\Phi_{mn}(k_{ymn}y)\cos(n\pi/b)z \tag{12}$$

where

$$\Phi_{mn}(k_{ymn}y) = A_{mn}\cos k_{ymn}y + B_{mn}\sin k_{ymn}y$$

and

$$\frac{k_x}{k} = \frac{1}{1-M^2}\{-M \pm [1-(1-M^2)\eta_{mn}{}^2]^{1/2}\} \tag{13}$$

$$\eta_{nm}{}^2 = (K_{ymn}/k)^2 + (n\pi/kb)^2; \qquad k = \omega/C$$

where ω is the driving frequency, c is the speed of sound in the air in the duct, M is the Mach number of the flow, $M = u/c$, d and b are the duct height and width, respectively. By assuming a normally reacting lining, Ingard's formulation of the boundary condition at a porous wall with grazing flow,[13] and the existence of a linear admittance model for the lining of the form $\bar{L} = \bar{L}(\omega,M)$, a solution for propagation, consisting of the superposition of individual modes of propagation, can be found in the form

$$p = \sum_m \sum_n \rho_{0mn} e^{i(\omega t - k_{xmn}x)}\Phi_{mn}(k_{ymn}y)\cos\frac{n\pi}{b}z \tag{14}$$

The wave numbers k_{xmn} are found as solutions to a transcendental eigenvalue equation dictated by the wall boundary conditions.[15]

A solution of this type will exist for solutions upstream and downstream of the noise source (inlet and exhaust flow). Since we assume an infinite duct the two types of solutions are not coupled because no termination reflections are permitted. The wave numbers k_{xmn} which correspond to downstream and upstream solutions are those which have negative and positive imaginary parts, respectively. If the imaginary parts are zero, as will occur for a rigid walled duct for modes which are not in the cutoff, then the appropriate solution can be determined by the phase velocity $(k/k_x)c$. The phase velocity should generally be positive for downstream propagation and negative for upstream propagation. However, for a given mode if $1 < \eta_{mn}{}^2 < (1-M^2)^{-1}$ in a rigid duct two negative phase velocities occur. Energy transmission considerations[27] show that the appropriate downstream solution is the one corresponding to the phase velocity obtained by choosing the positive sign in Eq. (13).

If we are interested in a solution for other than the least attenuated mode, the modal coefficients ρ_{0mn} in Eq. (14) are to be determined by forcing the series solution to satisfy the pressure field at some duct cross section, say $x = 0$. Presuming that experimental or assumed data is available from which we are able to extract the pressure fluctuations at frequency ω, we would define

$$\rho(y,z,t) = P(y,z)e^{i\omega t} \tag{15}$$

The pressure coefficients would then be required to satisfy

$$P(y,z) = \sum_m \sum_n \rho_{0mn}\Psi_{mn}(y,z) \tag{16}$$

where we have introduced $\Psi_{mn}(y,z)$ to denote the eigenfunctions. Since Ψ_{mn} are not orthogonal functions, unless the

walls are rigid or $M = 0$, we have used a collocation procedure to find ρ_{0mn} which utilizes a certain number of modes, say N, to satisfy Eq. (16) at N or more points on the cross section.

As noted previously, we presume that detailed pressure data is available at a given cross section. The type of data needed would involve the usual rms profile as well as time correlation to determine phases. If this type of information is not available, other assumptions are made regarding the modal content. For instance, it might be assumed that all modes not cutoff have equal amplitude or equal energy.

A theoretical figure of merit for the performance of the lining can be defined in several ways. The one which is most commonly used in the development program described here is the change of sound pressure level (SPL) over the lining length Δx

$$\Delta SPL = 20\,|\log\,[\rho(x + \Delta x)/\rho(x)]| \tag{17}$$

The pressure at x and $x + \Delta x$ would be evaluated at the same point on the cross section such as at the duct wall or at the duct center line.

Even this rather idealized model of the flow duct poses severe analytical and numerical problems. The prime challenge is the development of an efficient eigenvalue routine for the determination of the wave numbers, k_{xmn}. Early investigations[15] were directed toward one or two modes of propagation which combine to define the so called "least attenuated mode." These investigations established an efficient Newton-Raphson iteration procedure with an automated initial guess update procedure. This basic format has now been extended to a multi-mode capability with collocation for determining modal distribution.

Sheared Flow Profile

It has generally been presumed that the boundary layer in a duct has only a minor effect on the attenuation performance of acoustic linings. Considerable experience in the interpretation of flow duct test results has shown that the attenuations predicted by the uniform flow theory are generally higher than attainable in flow duct testing, particularly in the inlet flow. Although there are a number of ways in which the test facility violates the assumptions of the theory, we have focused attention on the boundary layer as a possible source of this discrepancy. To study the boundary-layer contribution we have employed the sheared flow method of Mungur and Gladwell[17] and Mungur and Plumblee[14] which are developed on the fundamental ground work of Tack and Lambert[4] and Pridmore-Brown.[12] The mathematical formulation of Mungur and Plumblee has been cast in a form utilizing a Newton-Raphson iteration scheme and automated initial guess update routine.[18] A capability is available for both the circular and annular duct. We have not developed a two-dimensional channel capability, since we have not ascertained the importance of the boundary layer on the adjacent walls which may affect the two-dimensional results.

As shown by Mungur and Plumblee,[14] the acoustic pressure distribution in a circular or annular duct with a sheared flow can be written:

$$\rho(r,\theta,x,t) = P(r)e^{i(\omega t - k_x x)} \cos m\theta \tag{18}$$

where $P(r)$ is defined by the ordinary differential equation

$$\frac{d^2P}{dr^2} + \left[\frac{1}{r} + \frac{2K}{1 - MK}\frac{dM}{dr}\right]\frac{dP}{dr} + k^2\left[(1 - MK)^2 - K^2 - \frac{m^2}{k^2r^2}\right]P = 0 \tag{19}$$

and $K = k_x/k$. The duct flow Mach number is the local mean flow Mach number defined by $M(r) = U(r)/c$.

In the circular duct case the duct wall at $r = R$ yields the boundary condition

$$dP/dr = -i\bar{L}_R k(1 - MK)^2 P; \qquad r = R \tag{20}$$

If the duct is annular we will have at the inner wall, $r = a$

$$dP/dr = i\bar{L}_a k(1 - MK)^2 P; \qquad r = a \tag{21}$$

The two-point boundary value problem is solved by the iterative Runge-Kutta integration method of Mungur and Gladwell.[17,18] In addition to the sinusoidal and constant gradient boundary-layer profiles generally assumed[14,17,18] we employ a closed-form integration in the boundary layer for very thin boundary-layer thicknesses and a partial closed-form integration in the $1/N$ power law boundary layer.

The current version of the sheared flow analysis program has multimodal capability for arbitrary angular or radial modes and uses a starting guess routine based on hard wall, $M = 0$, duct modes which eliminates all uncertainty about the migration of roots with frequency and Mach number. The computational efficiency of the sheared flow analysis is considerably less than the equivalent uniform flow case. For this reason this capability has been assigned a secondary role in the design procedure and is used to refine estimates of lining performance.

Optimization Programs

Both of the duct propagation mathematical models have associated with them optimization schemes used to define a lining impedance at the target frequency which provides the maximum attainable attenuation. As discussed previously we use a long duct philosophy and, consequently, place the greatest emphasis on the least attenuated mode of propagation in lining design. Thus, it has been considered to be both appropriate and efficient to define as optimum design based on a least attenuated mode solution to the governing duct equations.

In the case of the uniform flow model the procedure is analogous to that of Cremer[10] in the no flow case. An optimum impedance is one which causes two modes of propagation to coalesce. This means that we seek those values of impedance which lead to double roots of the eigenvalue equations generated by Eqs. (11), (12), and (13), or analogous relations. These double roots are termed saddle points and may be found by several means, as for example by Tester.[28] Tester points out that an optimum attenuation found in this way may actually reduce the attenuation in certain higher modes to such an extent that they, in reality, might become "least attenuated." His results were at fairly high frequency ($kl = 8\pi$) and we have not observed this at the lower frequencies at which we operate. However, this occurrence would not go unnoticed because of subsequent multimodal analyses in our design procedure.

Optimization in the case of sheared flow is performed directly by utilizing a steepest descent approach. This method is more versatile than the saddle point approach used in the uniform flow case in that the performance function to be optimized can represent attenuation in an arbitrarily weighted combination of modes. It is ordinarily used in a least attenuated mode format but several modes are continuously checked for minimum attenuation.

When the optimum wall impedance at the design point is determined, the mathematical model of the lining impedance is employed so that the appropriate physical parameters of the lining configuration which provide the required design point impedance can be specified.

Theoretical and Experimental Results

As noted previously, early flow duct testing of acoustic linings was undertaken with little or no theoretical backing, and what backing there was usually neglected the effect of the duct flow. However, a substantial body of test data showed rather consistent indications of a strong influence of the Mach number of the duct flow on the attenuation characteristics of

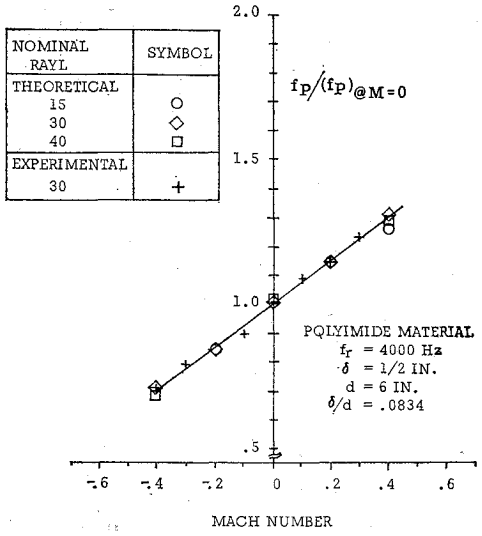

Fig. 8 Shift of tuning frequency due to duct flow.

the linings. The most consistent trend appeared in the frequency at which peak attenuation occurs in the attenuation spectrum. Figure (8) shows a normalized plot of the variation of the frequency of peak attenuation with Mach number, the frequency of peak attenuation being normalized with respect to conditions at $M = 0$. The experimental results are obtained by comparing insertion loss spectra at the various Mach numbers. The theoretical results are for attenuation spectra involving only the least attenuated mode. As noted by Eversman[18] this mode is actually a composite of two modes over the frequency range considered. At low frequencies, it is the fundamental mode and at higher frequencies it is a mode which at lower frequencies has a high attenuation.

Figure 8 shows comparisons with data obtained in the Boeing-Wichita facility on Polyimide type linings with an impedance characteristic modeled by

$$Z = (R/42)(1 + if/f_r) - i \cot k\delta \qquad (22)$$

where R is the flow resistance of the facing sheet, f is the driving frequency in Hertz, f_r the cross over frequency, $k = \omega/c$, and δ is the backing space depth. The comparison is very favorable for the conditions shown, even with the relatively crude impedance model.

Figure (9) shows attenuation spectra obtained in the Boeing-Wichita facility for 4% open area perforated sheet. The case shown is for a 32-in. panel on two walls in a 12in. by 9in. duct. The backing depth is 0.5in. and the distance between lined walls in 9in. Data were obtained in the inlet flow at $M = 0.15$ and 0.4, in the exhaust flow at $M = 0.2$, 0.4, and 0.6, as well as at $M = 0$. For comparison purposes theoretical results utilizing the uniform flow program and perforated plate mathematical model are shown. These results are based on an equal amplitude assumption for the modal distribution and include the plane wave across the hard walls and all soft wall modes not in cutoff. The equal-modal assumption was made in the absence of pressure profile information required for a collocation procedure. Although it is overly optimistic to say that excellent agreement is obtained, it is noted that some of the essential features are reproduced.

One noticeable trend which appears consistently in correlating theory and experiment is the overestimation of attenuation in the inlet mode at the higher Mach numbers. This has been explained, at least partially, by considering the effect of the boundary layer on attenuation. Reference 18 deals extensively with this problem, and it is found that the boundary layer can have a substantial effect on the deoptimization of lining performance, particularly in an inlet flow at high Mach numbers.

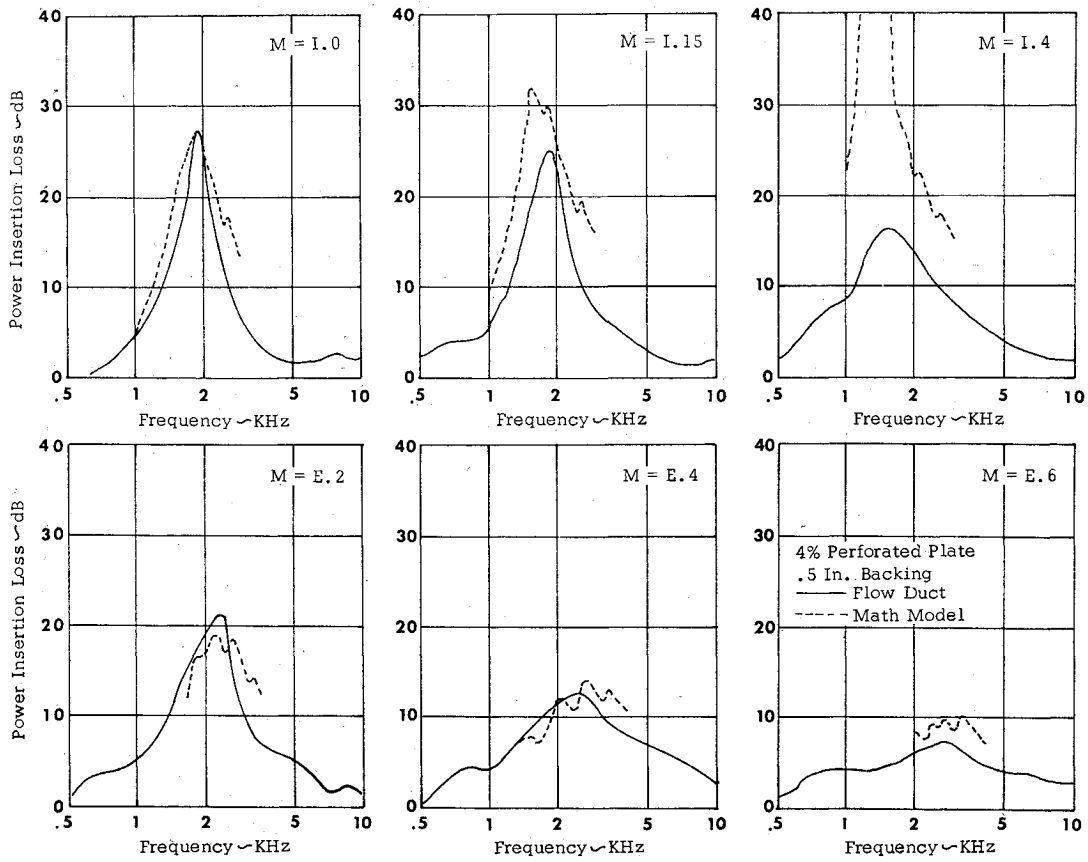

Fig. 9 Comparison of flow duct test results with theoretical multimodal results. Equal amplitude assumption.

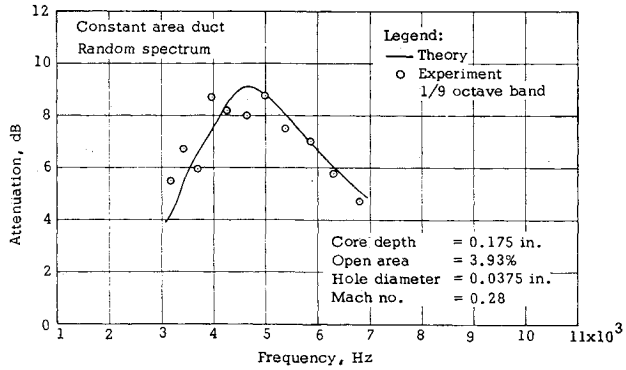

Fig. 10 Comparison of analytical predictions with flow duct test results for perforated sheet tailpipe lining design.

An excellent example of the validity of the analysis procedure was obtained from the design of acoustical treatment for the tailpipe of a JT3D-3B turbofan engine for the purpose of the reduction of turbine noise, as discussed in detail in Ref. 26. The lining design was tested in the flow duct with an input consisting of a broadband random spectrum at about 130 db SPL and a simulated turbine spectrum which was synthesized by vortex generators. Figure (10) shows the comparison between the measured attenuation spectrum and the spectrum computed theoretically. Theoretical design was based on a least attenuated mode optimization and the results shown were obtained from the uniform flow program on a multimodal basis, weighting the modal content for propagating modes on an equal amplitude basis. Since this is an exhaust flow case we expect only minor effects of boundary layer, and the results indicate excellent correlation.

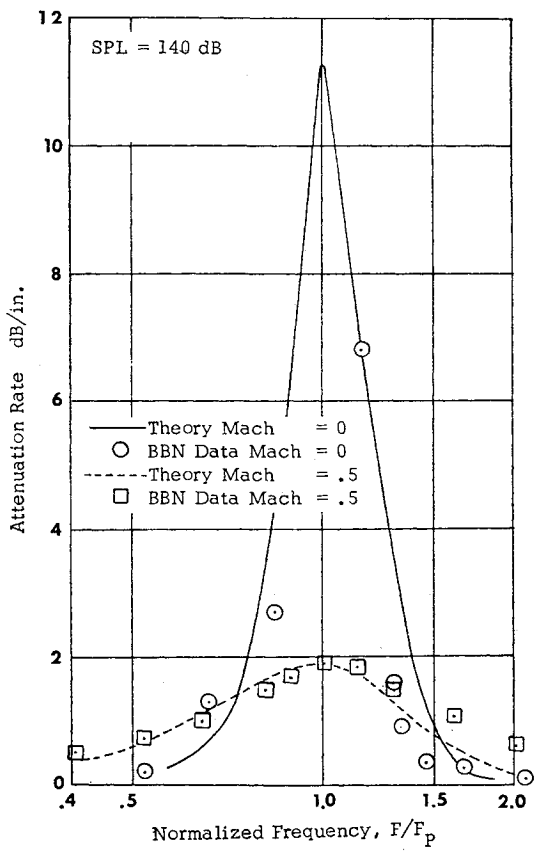

Fig. 11 Comparison of theoretical and experimental attenuations. Bolt, Beranek, and Newman data at 110 db, $M = 0$ and $M = 0.5$.

In order to further investigate the validity of the lining mathematical model and the duct analysis program, we have made computations corresponding to the conditions of a highly refined and closely controlled test performed and reported by Bolt, Beranek and Newman under contract to the Brunswick Corporation, Metal Fibers—Technical Production Division.[29] These tests were conducted in a 1in. × 1in. duct lined on one wall with 9.5% open area facing sheet on a 0.75in. backing space. Figure (11) shows results of the comparison at $M = 0.0$ and $M = 0.5$ at a driving SPL of 140 db. The frequency scale is normalized with respect to the frequency at which peak attenuation occurs F_p. It can be seen that the theoretical model matches all of the essential behavior observed in the test results. While a frequency by frequency comparison is ruled out by the normalization procedure, it can be stated that the normalizing frequencies found theoretically and experimentally were in satisfactory agreement.

Conclusions

We have indicated a rational procedure for the specification of design objectives for acoustic linings for turbo-fan noise suppression and the subsequent design and analysis phase. The design and analysis phases rest heavily on the interaction of a theoretical prediction capability and extensive flow duct testing. The mathematical models involved in the theoretical prediction have been discussed and results compared with appropriate experimental data. It has been found that, in general, the basic trends are predicted quite well, although comparison on a point by point basis leaves room for improvement in many areas. The reasons for discrepancies are not difficult to identify. The entire flow duct model is based on highly idealized equations of fluid motion. The flow duct facility probably violates nearly all of the basic assumptions. For example, the flow is highly turbulent, and the pressure fluctuations and gradients are large. In addition, the flow itself produces noise which establishes a noise floor and effectively reduces the attenuation capability of a given lining.

In spite of the problems associated with quantitative agreement of theory and experiment, we have found the combination to provide a highly efficient design procedure for the synthesis of acoustic linings which meet established design objectives.

References

[1] Federal Air Regulations, FAR Part 36.

[2] Meyer, E., Mechel, F., and Kurtze, G., "Experiments on the Influence of Flow on Sound Attenuation in Absorbing Ducts," *Journal of the Acoustical Society of America*, Vol. 30, No. 3, 1958, pp. 302–307.

[3] Mechel, F., Mertens, P., and Schliz, W., "Research on Sound Propagation in Sound Absorbent Ducts with Superimposed Airstreams," Rept. AMRL-TDR-62-140, Pts. I. II, III, and IV, 1962, U.S. Air Force Aerospace Medical Research Lab.

[4] Tack, D. H. and Lambert, R. F., "Influence of Shear Flow on Sound Attenuation in a Lined Duct," *Journal of the Acoustical Society of America*, Vol. 38, 1965, pp. 655–666.

[5] Mason, V., "Some Experiments on the Propagation of Sound Along a Cylindrical Duct Containing Flowing Air," *Journal of Sound and Vibration*, Vol. 10, No. 2, 1969, pp. 208–226.

[6] Marsh, A. H., "Study of Acoustical Treatments for Jet Engine Nacelles," *Journal of the Acoustical Society of America*, Vol. 43, No. 5, 1968, pp. 1137–1156.

[7] Eslinger, D. L., "The Boeing Wichita Acoustic Flow Duct Facility," Document D3-7993, Jan. 1969, The Boeing Co., Wichita, Kansas.

[8] Melling, T. H. and Doak, P. E., "Basic Design Considerations and Theoretical Analysis of Double-Reverberant Chamber Duct Lining Test Facilities," *Journal of Sound and Vibration*, Vol. 14, No. 1, 1971, pp. 23–25.

[9] Morse, P. M., "The Transmission of Sound Inside Pipes," *Journal of the Acoustical Society of America*, Vol. 11, Oct. 1939, pp. 205–210.

[10] Cremer, L., "Theorie der Luftschall-Dampfung in Rechtekkanal mit Schluckender Wand und das sich dabei Ergebende hochste Dampfungsmass," *Acoustica*, Vol. 3, 1953, pp. 249–263.

[11] Rice, E. J., "Attenuation of Sound in Soft Walled Circular Ducts," TM X-52442, 1968, NASA.

[12] Pridmore-Brown, D. C., "Sound Propagated in a Fluid Flowing in an Attenuating Duct," *Journal of Fluid Mechanics*, Vol. 4, 1958, pp. 393–406.

[13] Ingard, K. U., "Influence of Fluid Motion Past a Plane Boundary on Sound Reflection, Absorption, and Transmission," *Journal of the Acoustical Society of America*, Vol. 31, 1959, pp. 1035–1036.

[14] Mungur, P. and Plumblee, H. E., *Propagation and Attenuation of Sound in a Soft-Walled Annular Duct Containing a Sheared Flow*, NASA SP 207, July 1969, pp. 305–327.

[15] Eversman, W., "The Effect of Mach Number on the Tuning of an Acoustic Lining in a Flow Duct," *Journal of the Acoustical Society of America*, Vol. 48, No. 2 (Pt. 1), 1970, pp. 425–428.

[16] Doak, P. E. and Vaidya, P. G., "Attenuation of Plane Wave and Higher Order Mode Sound Propagation in Lined Ducts," *Journal of Sound and Vibration*, Vol. 12, No. 2, 1970, pp. 201–224.

[17] Mungur, P. and Gladwell, G. M. L., "Acoustic Wave Propagation in a Sheared Fluid Contained in a Duct," *Journal of Sound and Vibration*, Vol. 9, No. 1, 1969, pp. 28–48.

[18] Eversman, W., "The Effect of Boundary Layer on the Transmission and Attenuation of Sound in an Acoustically Treated Circular Duct," *Journal of the Acoustical Society of America*, Vol. 49, No. 5 (Pt. 1), May 1971, pp. 1372–1380.

[19] Green, L. and Duwez, P., "Fluid Flow Through Porous Metals," *Journal of Applied Mechanics*, Vol. 18, March 1951, pp. 39–45.

[20] Beranek, L., *Acoustics*, McGraw-Hill, New York, 1954, pp. 137–138.

[21] Phillips, B., "Effects of High-Wave Amplitude and Mean Flow on a Helmholtz Resonator," TMX-1582, May 1968, NASA.

[22] Zinn, B. T., "A Theoretical Study of Non-Linear Damping Characteristics of Helmholtz Resonators," AIAA Paper 69–481, Colorado Springs, Colo., 1969.

[23] Garrison, G. D. et al, "Suppression of Combustion Oscillations with Mechanical Damping Devices," PWA FR-3299, Aug. 1969, Pratt and Whitney Aircraft, East Hartford, Conn.

[24] Feder, E. and Dean, W. L. III, "Analytical and Experimental Studies for Predicting Noise Attenuation in Acoustically Treated Ducts for Turbofan Engines," CR-1373, Sept. 1969, NASA.

[25] Armstrong, D., "Acoustic Grazing Flow Impedance Using Wave Guide Principles," CR 120848, May 1972, NASA.

[26] Nelsen, M. D., Linscheid, L. L., Dinwiddie, B. A., and Hall, O. J., "Study and Development of Acoustic Treatment for Jet Engine Tailpipes," CR-1853, Nov. 1971, NASA.

[27] Eversman, W., "Energy Flow Criteria for Acoustic Propagation in Ducts with Flow," *Journal of the Acoustical Society of America*, Vol. 49, No. 6 Pt. 1, June 1971, pp. 1717–1721.

[28] Tester, J., "The Optimization of Sound Attenuation in Lined Ducts Containing Uniform, Axial, Subsonic, Mean Flow," Paper 20 P7, Seventh International Congress on Acoustics, Budapest, 1971.

[29] Kurze, U. J. and Allen, C. H., "The Attenuation in Ducts Lined with Perforated Plate," BBN Job 151576, Progress Rept. No. 5, Sept. 1969, Bolt, Beranek, and Newman, Cambridge, Mass.

AUGUST 1972 J. AIRCRAFT VOL. 9, NO. 8

Closed Form Solution for the Sonic Boom in a Polytropic Atmosphere

R. STUFF*

Deutsche Forschungs- und Versuchsanstalt für Luft- und Raumfahrt, Aachen, Germany

The sonic boom problem for typical aircraft maneuvers in a polytropic atmosphere is solved analytically using the analytic method of characteristics. The linearized wave propagation, which serves as initial solution to the method of characteristics, is solved first. The velocity perturbations are multiplied by the factor $(c_{op}p_{op}/c_op_o)^{1/2}$. With c_o as local sound velocity and p_o as local static pressure, the product c_op_o is, per unit time, the work done by the static pressure at local altitude, and $c_{op}p_{op}$ is the corresponding quantity at flight altitude. The characteristic method is modified to encompass the case of an oncoming stream with variable sound velocity.

Nomenclature

A = coefficient of sound-velocity statification
B = acceleration coefficient
b = acceleration
c = speed of sound
F = Whitham's F function
G = distance function
g = gravity acceleration
K_r = curvature of the envelope
$K_{1,2}$ = constants of integration
l = body length
M = Mach number related to c_{op}
m = gradient of the speed of sound
p = pressure
R_K = radius of curvature of the flight path
R = instantaneous radius of the wave front
s = ray
t = time dimensionless by l and c_{op}
u = velocity vector
x, y, z = rectangular coordinates dimensionless by l
x = axial coordinate
z = vertical coordinate
α = coefficient of gravity stratification
γ = ratio of specific heats
η = coefficient of polytropic stratification

Received October 12, 1971; revision received April 28, 1972.

Index categories: Aerodynamic and Powerplant Noise (Including Sonic Boom); Aircraft Flight Operations; Supersonic and Hypersonic Flow.

*Research Scientist, Institut für Theoretische Gasdynamik.